Characterizing Brazilian Fires and Estimating Areas Burned by Using the Airborne Infrared Disaster Assessment System

James A. Brass, Liane S. Guild, Philip J. Riggan, Vincent G. Ambrosia, Robert N. Lockwood, João A. Pereira, and Robert G. Higgins

Biomass burning is a common force in much of the developing tropical world and has wide-ranging environmental impacts. Fire is an important component in tropical deforestation and is often used to clear broad expanses of land for shifting agriculture, dispose of crop residue, and "clean" pastures for cattle grazing. It is part of a complex social phenomenon driven by human population expansion, national economics, foreign debt, land speculation, tax incentives, colonization, and political forces (Fearnside 1987; Hecht and Cockburn 1990). Biomass burning has an important role in the annual fluxes to the troposphere of many trace gases (Crutzen et al. 1979). However, only rough estimates of the contribution of biomass burning to the tropospheric trace-gas budget are available (Robinson 1988). In this chapter we present the capabilities and limitations of satellite data for characterizing biomass combustion. A new aircraft scanner technology is discussed that incorporates high resolution, extended dynamic range, and high-temperature calibration. Data obtained during a prescribed fire in the Brazilian cerrado are used to demonstrate the system's capabilities and to characterize important fire parameters for issues of global change.

The greatest source of fire emissions is probably tropical fires, including fires in natural ecosystems and fires to clear agricultural land (Seiler and Conrad 1987; Crutzen et al. 1985; Robinson 1988; Crutzen and Andreae 1990). Biomass combustion may be a major source of the radiation-absorbing gas methane (CH_4) and other greenhouse gases. Measurements in North America have shown that fire emissions are also a strong global source of some nongreenhouse gases, such as carbon monoxide (CO) and nitric oxide (NO), which affect the rate at which methane is removed from the atmosphere, and ammonia (NH_3), which is a major source of nitrogen deposition in downwind areas (Hegg et al. 1988; 1990). Andreae (1991) Indicates that the uncertainty of these estimates is about 50% for carbon species (where emissions are relatively well known) and about a factor of two for most other gases.

A major cause of uncertainty in determining the contribution of biomass combustion to trace-gas generation and environmental impacts is the extent of area burned, intensity of the fire, and rate of spread, especially in tropical ecosystems (Seiler and Crutzen 1980; Matson and Ojima 1990; Robinson 1988). Current predictions on the contribution of trace gases to the atmosphere are based in part on population estimates for shifting agricultural areas multiplied by records of area burned per family unit. The records of burn area per family unit and population statistics are inaccurate at best (Robinson 1988). The estimate of burned area per family is also suspect, for the acreage is extrapolated from few actual measurements, which are highly variable depending on region of Brazil, cropping practices, and charcoal production (personal communication, B. Dias, 1993, Ministry of Environment, Brazil).

Robinson (1988) has examined the uncertainty in the computation of global emissions from biomass burning with the equation provided by Seiler and Crutzen (1980). Global carbon emissions were calculated in table 54.1 using this equation:

$$\text{Emissions}_r \text{ (mass per time)} = \Sigma_r(A_r^* B_r^* a_r^* b_r^* ef_s) \qquad (54.1)$$

where

A_r is the area burned

B_r is the biomass per unit area

a_r is the consumption of biomass

b_r is the fraction of aboveground biomass

$_r$ is the region of interest

ef_s is the emission factor for the species (s)

This calculation illustrates the parameters currently used to determine emissions from fire and reveals the large uncertainty in current knowledge. These parameters of emission estimates are known to have variances of $\pm 30\%$ of their means, and some measurements such as fuel consumption and area burned, are no better than $\pm 50\%$ (Andreae 1991; Robinson 1988; Seiler and Conrad 1987). These estimates, however,

Table 54.1 Global estimates of carbon emissions from biomass burning (adapted from Robinson 1988)

Source	Estimated emissions (10^{15} g C yr^{-1})
Study of Man's Impact on Climate (1971)	0.13–0.64
Wong (1978)	5.6
Seiler and Crutzen (1980)	2–4
Olson (1981)	3.2–6.8
Logan et al. (1984)	3.4

are the only data available for tropospheric chemistry and global-change modeling. To reduce the uncertainties in biomass combustion estimates, research has turned to remote sensing for judging extent and characterization of fires.

Myers (1989) and Brustet et al. (1991) acknowledged the importance of satellite and airborne remote-sensing technology in providing better estimates of burn area and fire intensity. Brass (1995) summarized the measurable fire parameters from remote sensing as three very different signals: the fireline itself produces thermal and visible signals; smoke and aerosols from volatilization produce an optical signal; and char produces a characteristic spectral signature in the visible and thermal infrared. These results of biomass combustion must be characterized remotely if fire emissions and, ultimately, fire impacts are to be estimated.

Satellite Remote Sensing

As with many global-change issues, Riggan et al. (1993) suggest that synoptic measurements on a regional and global scale are needed to determine the magnitude of combustion emissions and fire effects. Fire emissions from a source region can be estimated as the time-integrated product of (1) area burned per unit of time, (2) biomass consumption per unit area, and (3) emissions per mass consumed (emission factor). Remote sensing can possibly provide an estimate of regional fire growth, depending on the system's resolution (both spatial and temporal). Remote measurements can also be made to estimate the fire's radiant energy flux, a possible predictor of biomass consumption rate. Current satellite systems must be examined to determine the applicability of these space-based instruments for mapping and characterizing fires.

The Geostationary Operational Environmental Satellite (GOES) Visible Infrared Spin Scan Radiometer Atmospheric Sounder (VAS), using 3.9 and 11.2 micrometer (μm) windows, has been used to detect fires and to estimate their size and temperature. Fire detection is accomplished with a threshold technique on both channels following calculation of haze-corrected brightness temperatures. This satellite's temporal resolution (i.e., data every half hour), means that small fires can be visually detected by the occurrence of smoke plumes. Menzel et al. (1991) report, however, that because of the system's limited resolution (0.9 km visible, 13.8 km in the 3.9-μm channel, and 6.9 km in the 11.2-μm channel), many small fires are missed, and burned-area estimates are accurate only within a factor of two compared to other sensor systems. Fire-temperature predictions are also inaccurate, because the spatial resolution of the instrument results in averaging of flaming, smoldering, and background temperatures. The highly temporal information received from GOES enables diurnal sensing of fire activity. Menzel et al. (1991) have shown that in Brazil most fires occur between 1230 and 1530 local time. Menzel et al. (1991) have also shown that aerosol transport can be tracked accurately with the GOES.

Orbiting satellite systems such as the National Oceanic and Atmospheric Administration's Advanced Very High Resolution Radiometer (AVHRR) and the Thematic Mapper (TM) carried by the Landsat series of satellites, have been used for monitoring fires. The large area covered by the AVHRR system and its two daily passes (two satellites; four passes) provide an operational framework for fire detection. Resolution of the AVHRR ranges from 1 km in local area coverage (LAC) mode to 4 km in global area coverage (GAC) mode. Channels in the infrared, such as channel 3 (3.55–3.95 μm) responding to both reflected solar and emitted radiation, have been used singly or in combination with shorter-wavelength channels to characterize fire occurrence and temperature (Setzer and Pereira 1991).

Active fires are a complex target for any remote-sensing system with the resolution to discriminate individual flamefronts. This burning can be characterized as a gradient of temperatures and radiances from spreading firefront to residual flaming, smoldering combustion, and cooling ash (Riggan et al. 1993). Peak temperatures measured 1 m above the ground can range from 1300 K in chaparral (F. Weirich, unpub. report, 1993, USDA Forest Service, Riverside, California) to 900 K in Brazilian savanna (A. Miranda, 1994, personal communication). Ash surfaces in chaparral can remain above 700 K for one to two min following the flamefront, and under solar heating they reach temperatures as high as 345 K (Riggan et al. 1993). Flames and ash at peak temperatures are very bright targets in the intermediate infrared wavelengths. For example, blackbody radiation at 1173 K is maximized at 2.5 μm. But at 11 μm, this same blackbody radiation is 38 times as great as that emitted at common terrestrial (background) temperatures.

The local area coverage (1 km) and global area coverage (4 km) of the AVHRR have been used successfully for detecting fires. However, they have been found to saturate in band 3 over actively burning areas because of the radiance produced by flame and hot ash. This saturation problem prevents any calculation of fire intensity or accurate description of flamefront size and smoldering area. Specular reflection from bare ground and dry foliage produces bright targets in band 3, resulting in false positives for fire detection. In Brazil, this problem is quite evident in the Caatinga region, where overestimates of fire activity are often seen (A. Setzer, 1994, personal communication).

The higher-resolution, lower-orbit Landsat series of satellites offers ability to monitor fire activity in shortwave and longwave infrared channels. Using the TM sensor onboard both Landsats 4 and 5, 30-m data (120-m thermal infrared) are collected every 16 days. Channels 5 (1.65 μm), 6 (11.5 μm), and 7 (2.2 μm) provide most of the information for active fire characterization. The 1.65- and 2.2-μm channels are particularly effective for mapping burn scars. However, using only a thresholding technique for scar detection requires local knowledge of scar characteristics and some spectral training (see Hlavka et al., chapter 53 this volume).

Landsat TM data continue to be used for describing and mapping actively burning fires. The area and temperature of the flamefront within a pixel can be estimated using two wavelengths, and if the target behaves as a blackbody, the radiance of the background can be estimated from nearby pixels and the signal does not saturate the system detectors (Matson and Dozier 1981). However, upwelling radiation common in large fires will saturate TM channels 6 and 7 detectors (A. Setzer, personal communication; Brustet et al. 1991). Therefore, a statistical distribution of fire radiances derived from TM would be biased (Riggan et al. 1993). Any attempt to use the binary algorithm (fire and background) posed by Matson and Dozier (1981) when a pixel encompassed the active firefront, ash layer, and background would result in the Planck Function evaluated at the composite temperature, a poor estimator of fire size and temperature.

Airborne Remote Sensing

Brustet et al. (1991) recommend examining remote sensing of fires from aircraft to better understand fire. A number of airborne systems have been used to detect and map fires. A majority of these systems are prototypes of satellite systems currently in operation for general land-use/land-cover mapping. Generally, these linescanning systems collect data in broad bands using low-temperature blackbodies onboard for calibration. Historically, these systems had numerous problems when used to measure radiances from active fires. Following Wein's Displacement Law, the peak radiant emittance for temperatures of 900 K occurs between 3.0 and 4.0 μm, and for ambient earth temperatures, between 10.0 and 11.0 μm. Airborne systems are usually not optimized for characterizing fire because they lack channels in this part of the electromagnetic spectrum.

Calibration, as required for active fire characterization, is a second problem encountered by an airborne scanner system. Ambrosia and Brass (1988) document the problems with onboard calibration and the relationship of brightness to temperature based on two low-temperature blackbodies. As evidenced by Planck's function, the linear relationship defined by the blackbodies does not hold for temperatures produced by active firefronts and superheated soils.

Signal saturation is the third problem area found in many airborne systems. As discussed earlier, radiance from active fires can be 50 times that found at ambient temperatures. Many times the dynamic range of the system cannot process both an ambient signal and a high-radiance signal from fire. For airborne systems flying for earth-science research, fires were not considered in the original design; this lack has resulted in detector saturation levels of 90 to 100°C (Ambrosia and Brass 1988). Fire-detection and burn-area estimating are certainly possible with these systems. However, firefront dimensions, fire temperature, and fire intensity cannot be derived from the saturated data set (Brass et al. 1987).

Instrument Development—AIRDAS

The Airborne Infrared Disaster Assessment System (AIRDAS) is a new airborne scanner specifically designed by NASA and U.S. Forest Service (USFS) for fire characterizing and fuel mapping. This spectrometer incorporates the chassis and optical system of a Texas Instruments RS-25 thermal linescanner. It is a 4-channel, 16-bit system with detectors of silicon (Si),

Table 54.2 AIRDAS Initial configuration

Channel	Detector	TM band simulation	Wavelength (in μm)
1	Si	3	0.64–0.71
2	InGaAs	5	1.57–1.70
3	InSb		3.75–4.05
4	N_gCdTe	6	5.5–12.5

indium-gallium arsenide (InGaAs), indium antimonide (InSb), and mercury-cadmium telluride (NgCaTe). An initial configuration with channels placed throughout the visible and thermal infrared is shown in table 54.2.

The field of view of the scanner is 108° cross-track with an instantaneous field of view of 2.62 milliradians. At 3000-m altitude, a ground resolution of 7.8 m is realized. The data are stored on exabyte tapes with 5-gigabyte capacity. The system contains its own global positioning system (GPS) and real-time visualization capability. The data are roll-corrected using postflight software.

The three infrared channels of the spectrometer have been calibrated in the laboratory to temperatures above 900 K. The target used for calibration consists of a 23 × 48 × 0.6-cm plate treated with a solar-absorbing coating with a known emissivity of 0.95. The target is heated from below by an array of quartz heaters with nine thermocouples on the plate surface to characterize the target temperature.

Fire Characterization

The AIRDAS spectrometer has been deployed in Brazil three times in the last four years to support a large, multiagency global-change research program. The most recent mission, in August 1994, had four objectives:

1. Determine the relationship between fire emissions and the fire's physical properties using remote sensing and air sampling;

2. Examine physical properties of fires in major biomes;

3. Characterize the extent and progession of burning with high-resolution remote sensing;

4. Determine the impact of Brazilian fires on global-change issues such as nutrient movement and trace-gas generation.

The AIRDAS spectrometer was deployed to Central Brazil and mounted in a Lear Jet Model 35. Prescribed and wildland fires were overflown to meet the August 1994 objectives. Of particular importance was the prescribed fire at the Reserva Ecologica of the Instituto Brasíleiro de Geografia e Estatistica (IBGE) near Brasília. This fire, located in the *campo limpo* (clean field) form of cerrado, or savanna vegetation, was ground-instrumented for fire and soil temperature and wind speed and direction, and biomass was measured prior to and following the burn. The campo limpo fire was planned for a perimeter ignition of 200 ha; however, a wildfire to the north crossed control lines and ignited the prescribed burn area in the ecological reserve.

Multiple passes were made over the fire with the AIRDAS spectrometer. The instrument provided data documenting fire behavior, flaming and smoldering stages, rate of spread, and burned-area progression. Figures 54.1, 54.2, and 54.3 illustrate the movement of the firefront (north is at the top) as it burned through the grassland with an average fuel loading of 0.65 kg/m^2 (Kauffman et al. 1994). The fireline spread in two primary directions, one nearly parallel to the wind, as evidenced by the direction of the smoke movement, and one running with the wind. Flame temperatures were similar between the two lines, but the energy release rate was several times greater from the fireline running with the wind, as evidenced by the size of the flamefront recorded by the AIRDAS. Residual combustion was also apparent along the gallery forest and small riparian zones, as shown in figure 54.3. Estimated fire temperatures calculated using methodology developed by Riggan et al. (1993) were within expected values of between 930 K and 1340 K, which compared well with thermocouple data taken near the ground (Miranda et al. 1994). The soil surface radiated little energy following passage of the flamefront as pixels behind the flames quickly cooled nearly to ambient temperatures. Radiances of cooled ash in the 1.65-μm channel were less than 2% of those measured in the flaming zone.

The infrared data collected during the 18 passes over the fire provided valuable information on rates of consumption during the combustion phase. The multispectral images collected during each pass were spatially corrected for aircraft attitude and scanner geometry. Following preprocessing of the data, consumption was calculated using a comparative analysis—subtracting the burn area estimated from one image from the burn area estimated from a second (later) image. To derive the burn area, a spectral threshold was applied to the images after training on both burned and unburned areas. The consumption

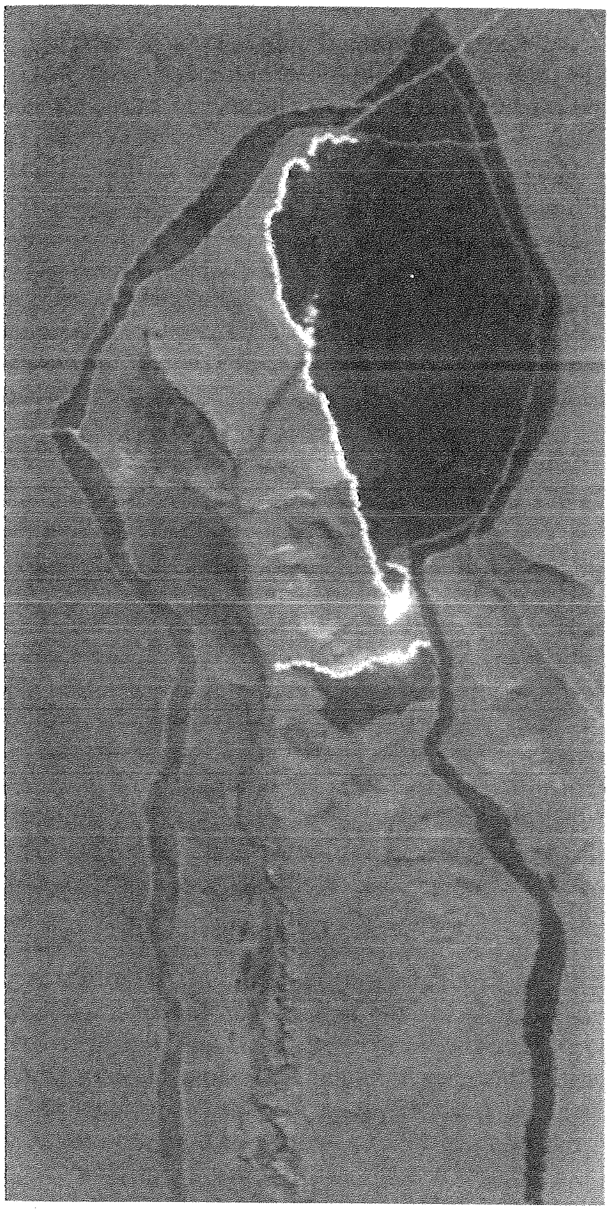

Figure 54.1 AIRDAS image collected over the IBGE ecological reserve near Brasília, Brazil, at 1552 local time. This 1.57–1.70 μm channel displays the active fire front in white, with the burn scar in black. The major fireline is burning parallel to the wind, hence flame lengths are small, resulting in a narrow fireline.

Figure 54.2 AIRDAS image collected over the IBGE ecological reserve near Brasília, Brazil, at 1625 local time. This 1.57–1.70 μm channel displays the active fire in white. The wide portions of the fireline are more intensely burning areas caused by the fire being propagated by the wind.

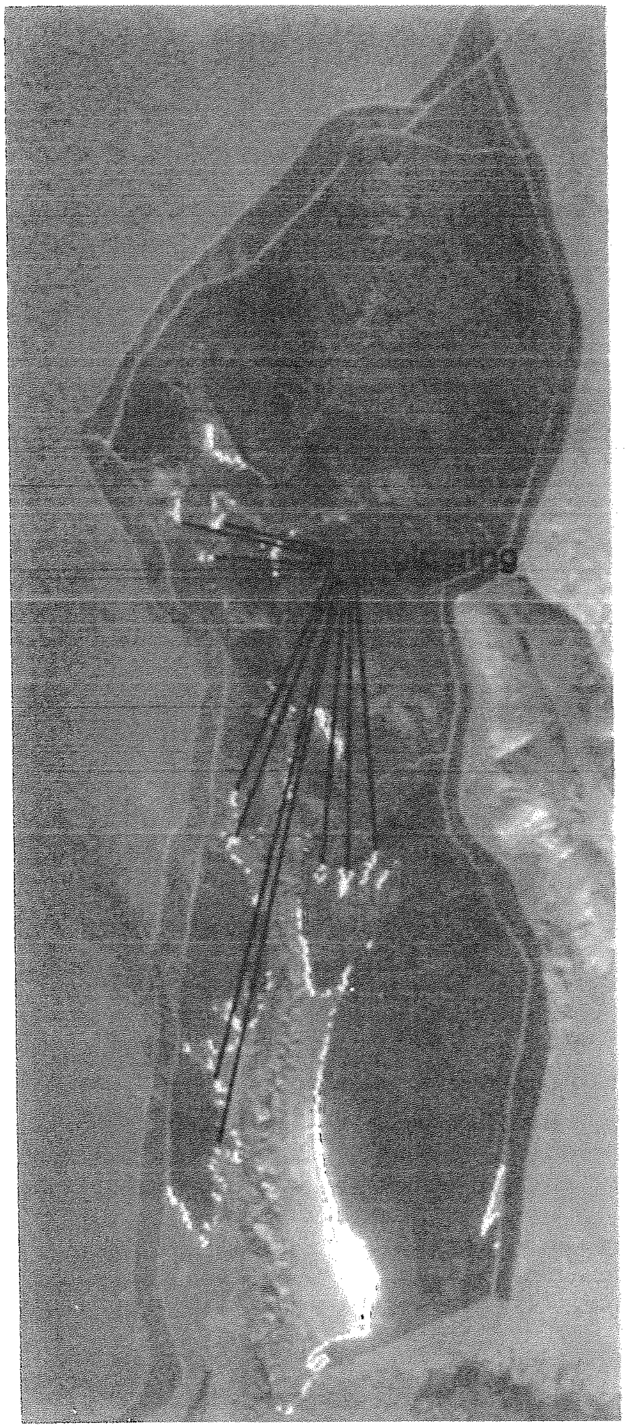

Figure 54.3 AIRDAS image collected over the IBGE ecological reserve near Brasília, Brazil, at 1714 local time. This 1.57–1.70 μm channel displays flaming and smoldering combustion during this stage of the fire. Using the infrared channels collected over this fire, the discrimination of flaming versus smoldering (marked on image) was accomplished.

during the first 30 min of the fire was found to be 32.3 kg of biomass (primarily grass), with rates of spread ranging from 0.1 to 3 m/sec. The variability in the rates of spread was due primarily to wind speed and to a lesser extent topography, for the terrain can be described as gently sloping to the south and west (Miranda 1994).

Several factors influence biomass burning emissions. According to Lobert et al. (1991), the most important effect has been identified as the kind and duration of burning stage. The AIRDAS multispectral system provides unsaturated data characterizing flaming and smoldering conditions. Figures 54.1, 54.2, and 54.3 illustrate differing amounts of smoldering activity. The flaming stage dominated by hot combustion with open flames can be discriminated from cooler incomplete combustion without flames (smoldering). Figure 54.1 is an example of a fire dominated by flaming combustion, where temperatures along the fireline range between 850 K and 1150 K. Little residual combustion is evident behind the active firefront, with most gases being flaming-stage compounds (i.e., CO_2, NO_x, N_2O). Comparing figure 54.1 with figure 54.3, the flaming activity in the later image was much less homogeneous. It is evident that many small patches of smoldering combustion appear behind and above (north) the active firefront. Here, one would expect the combustion to produce smoldering-stage gases such as CO, C_2H_6 (ethane), and C_2H_4 (ethene).

Examining the multiple aircraft passes over this savanna fire, it is evident that combustion changed markedly during the burn, with flaming dominating the combustion in some stages of the fire (figure 54.1) and smoldering dominating combustion in others (figure 54.3). Within figure 54.3, we have calculated the flaming combustion to be 1.8% of the burn area, and smoldering to be 2.1% of the burn area. It is important to note that during this stage (figure 54.3) of the fire, a greater percentage of smoldering was taking place. These differences in combustion must be accounted for when attempting to predict trace-gas generation from fires in the cerrado of Brazil.

Conclusion

Biomass burning is an important component in the annual fluxes of trace gases to the troposphere. The tropics have been identified as a major source of these trace gases. However, only rough estimates of the contribution by burning to the tropospheric trace-gas budget are available. Remote sensing continues to play a role in characterizing the numbers, size, and intensity of these fires. However, satellite-based systems have been shown to be of limited value when actual numbers, size, and intensity of burning are required.

The Airborne Infrared Disaster Assessment System (AIRDAS) brings unique capabilities for assessing fire impacts on terrestrial and atmospheric processes. The dynamic range and high-temperature calibration of this instrument allow fire radiance and firespread calculations to be made, these calculations being critical parameters for predicting trace-gas generation.

Research flights during August 1994 over the Brazilian cerrado have provided the scientific community with the first extensive data set characterizing fires and fire occurrence. The prescribed/wildland fire examined here provides a first look into the characteristics of fires in the campo limpo ecosystem. The data from multiple passes over the fire have shown the large variability in fireline movement and intensity in this homogeneous fuel type. These unique remote-sensing data have been used to document stage in combustion and illustrate the importance of smoldering combustion in this ecosystem.

The 1994 Brazilian campaign measured more than 150 fires in the cerrado region. This data set is currently being analyzed for fire size, intensity, consumption, and location. In this chapter we have attempted to characterize one of those fires as an indication of the general characteristics found among other fires in the campo limpo. Remote-sensing systems designed specifically for monitoring fire are continuing to exert great influence in characterizing important combustion characteristics in this fire-dominated ecosystem, and they must be a component in the overall approach to predicting fire impacts on atmospheric and terrestrial processes both locally and regionally.

Acknowledgments

This research was supported by the global change research programs of the U.S. Agency for International Development, and USDA Forest Service, and NASA's Mission to Planet Earth program. We wish to thank Dr. Heloisa Miranda, Dr. Antonio Miranda, and Maria Iracema Gonzales and staff from the Reserva Ecologica do IBGE for their contributions to research in Brazil; James Allen and Dr. Edward Hildum for their design, development, and support of the AIRDAS, and Susan Alexander, Louisa Beck, Chris Hlavka, Lee Johnson, and Brad Lobitz for their perseverance in reviewing this chapter. Finally, we would like to thank Lee Mikula for her technical assistance in preparing the chapter.

References

Ambrosia, V. G., and J. A. Brass. 1988. Thermal analysis of wildfires and effects on global ecosystem cycling. *Geocarto Int'l.* 3, (1), 29–39.

Andreae, M. O. 1991. Biomass burning: Its history, use and distribution and its impact on environmental quality and global change, Chapter 1 in J. S. Levine (Ed.) *Global Biomass Burning*, MIT Press, Cambridge, Mass.

Brass, J. A. 1996. Fires and global change: Prospects for remote sensing assessment. In *World Resources Review*, in press.

Brass, J. A., V. G. Ambrosia, P. J. Riggan, J. S. Myers, and J. C. Arvesen. 1987. Aircraft and satellite thermographic systems for wildfire mapping and assessment, *AIAA*, 87–0187.

Brustet, J. M., J. B. Vickos, J. Fontan, A. Podaire, and F. Lavenu. 1991. Characterization of active fires in West African savannas by analysis of satellite data: Landsat Thematic Mapper, chapter 6 in J. S. Levine, ed., *Global Biomass Burning*, MIT Press, Cambridge, Mass.

Crutzen, P. J., L. E. Heidt, J. P. Krasner, W. H. Pollock, and W. Seiler. 1979. Biomass burning as a source of atmospheric gases CO, H_2, N_2O. *Nature* 282, 253–256.

Crutzen, P. J., A. C. Delany, J. Greenberg, P. Haagenson, L. Heidt, W. Pollock, W. Seiler, A. Wartburg, and P. Zimmerman. 1985. Tropospheric chemical composition measurements in Brazil during the dry season. *J. Atmos. Chem.* 2, 233–256.

Crutzen, P. J., and M. O. Andreae. 1990. *Science* 250, 1670–1678.

Dias, B. 1993. Ministry of Environment, personal communcation, Brazil.

Fearnside, P. M. 1987. Cause of deforestation in the Brazilian Amazon. In R. E. Dickinson, ed., *The Geophysiology of Amazonia—Vegetation and Climate Interactions*, John Wiley, New York, pp. 37–61.

Hecht, S., and A. Cockburn. 1990. *The Fate of the Forest*, Harper, New York, 358 pp.

Hegg, D. A., L. F. Radke, P. V. Hobbs, J. H. Lyons, and P. J. Riggan. 1990. Emissions of some trace gases from biomass fires. *J. Geophys. Res.* 95, 5669–5675.

Hegg, D. A., L. F. Radke, P. V. Hobbs, and P. J. Riggan. 1988. Ammonia emissions from biomass burning, *Geophys. Res. Letters* 15, 335–337.

Kauffman, J. B., R. W. Shea, R. F. Hughes, D. L. Cummings, E. A. Castro, and R. D. Ottmar. 1995. Total aboveground biomass, fuel loads and combustion factors of Brazilian tropical forests and savannas. *J. Ecol.*, submitted.

Lobert, J. M., D. H. Scharffe, W. M. Hao, T. A. Kuhlbusch, R. Seuwen, P. Warneck, and P. J. Crutzen. 1991. Experimental evaluation of biomass burning emissions: nitrogen and carbon-containing compounds. Chapter 36 in *Global Biomass Burning*, MIT Press, Cambridge, Mass., pp. 289–304.

Matson, M., and J. Dozier. 1981. Identification or subresolution high temperature sources using thermal IR sensor, *Photo Eng. and Remote Sensing* 47, (9) 1311–1318.

Matson, P. A., and D. Ojima. 1990. Terrestrial biosphere exchange with global atmospheric chemistry, IGBP Report No. 13, Stockholm, 103 pp.

Menzel, W. P., E. C. Cutrim, and E. M. Prins. 1991. Geostationary satellite estimation of biomass burning in Amazonia during BASE-A. Chapter 4 in J. S. Levine (ed.), *Global Biomass Burning*, MIT Press, Cambridge, Mass.

Meyers, N. 1989. The greenhouse effect: A tropical forestry response, *Biomass* 18, 73–78.

Miranda, A. 1994. University of Brasília, personal communication. Brazil.

Miranda, A., H. S. Miranda, I. F. D. Dias, and B. F. S. Dias. 1994. Soil and air temperatures during prescribed Cerrado Fires in Central Brazil. *J. of Trop. Ecol.* 9.

Riggan, P. J., J. A. Brass, and R. N. Lockwood. 1993. Assessing fire emissions from tropical savannas and forests of Central Brazil. *Photo. Eng. and Rem. Sensing* 59, 6, 1009–1015.

Robinson, J. M. 1988. The role of fire on earth: a review of the state of knowledge and a systems framework for satellite and ground-based observations, Cooperative Thesis No. 112, University of California, Santa Barbara, and National Center for Atmospheric Research.

Seiler, W., and P. J. Crutzen. 1980. Estimation of gross and net fluxes of carbon between the biosphere and the atmosphere from biomass burning, in *Climatic Change, 2*, 207–247.

Seiler, W., and R. Conrad. 1987. Contribution of tropical ecosystems to the global budgets of trace gases, especially CH_4, H_2, CO and N_2O, Chapter 9 in R. E. Dixon, ed., *The Physiology of Amazonia*, John Wiley, New York.

Setzer, A. 1994. INPE, personal communication, Brazil.

Setzer, A., and M. Pereira. 1991. Amazonia biomass burnings in 1987 and an estimate of their tropospheric emissions. *Ambio* 20, (1).

Weirich, F. 1993. Unpublished report, USDA Forest Service, PSW For. and Range Exp., Sta., Riverside, Calif.